Optimized Schwarz Method for the fluid-structure interaction with cylindrical interfaces

Giacomo Gigante[1] and Christian Vergara[2]

1 Introduction

The Optimized Schwarz Method (OSM) is a domain decomposition method based on the introduction of generalized Robin interface conditions obtained by linearly combining the two physical interface conditions through the introduction of suitable symbols, and then on the optimization of such symbols within a proper subset, see Lions [1990], Japhet [1998]. This method has been considered so far for many problems in the case of flat interfaces, see, e.g., Gander [2006], Japhet et al. [2001], Gander et al. [2002], Qaddouria et al. [2008], Dolean et al. [2009], Gerardo Giorda et al. [2010], Stupfel [2010]. Recently, in Gigante et al. [2013], Gigante and Vergara [2013], OSM has been considered and analyzed for the case of cylindrical interfaces. In particular, in Gigante and Vergara [2013] we developed a general convergence analysis of the Schwarz method for elliptic problems and an optimization procedure within the constants, with application to the fluid-structure interaction (FSI) problem.

In this work, we provide a numerical study of the performance of the optimization procedure developed in Gigante and Vergara [2013] for the FSI problem when the solution is characterized by non-null angular frequencies, thus breaking the radial symmetry. The reported 3D numerical results for a cylindrical domain showed the effectiveness of the procedure proposed in Gigante and Vergara [2013] also in such a case.

The outline of this paper is as follows. In Section 2 we report the convergence result developed in Gigante and Vergara [2013] with application to the FSI problem, whereas in Section 3 we describe the optimization procedure. Finally, in Section 4 we show the numerical results.

[1] Dipartimento di Ingegneria, Università di Bergamo, Viale Marconi 5, 24044, Dalmine (BG), Italy giacomo.gigante@unibg.it · [2] Dipartimento di Ingegneria, Università di Bergamo, Viale Marconi 5, 24044, Dalmine (BG), Italy christian.vergara@unibg.it

2 Convergence analysis

We consider the interaction between an incompressible, inviscid and linear fluid in the cylindrical domain $\Omega_f := \{(x, y, z) \in \mathbb{R}^3 : x^2 + y^2 < R^2\}$, for a given $R \in \mathbb{R}^+$, and a linear elastic structure described by the wave equation in the cylindrical crown $\Omega_s := \{(x, y, z) \in \mathbb{R}^3 : R^2 < x^2 + y^2 < (R + H)^2\}$, with H the structure thickness. The two subproblems interact at the common cylindrical interface $\Sigma_R = \{(x, y, z) \in \mathbb{R}^3 : x^2 + y^2 = R^2\}$. We also introduce the cylindrical variables r, φ defined by $x = r\cos\varphi$ and $y = r\sin\varphi$. After the time discretization obtained with a BDF1 scheme for both subproblems, the coupled problem at time $t^{n+1} := (n+1)\Delta t$, Δt being the time discretization parameter, reads

$$\begin{cases} \rho_f \delta_t \boldsymbol{u} + \nabla p = \boldsymbol{0} & \text{in } \Omega_f, \\ \nabla \cdot \boldsymbol{u} = 0 & \text{in } \Omega_f, \\ \int_{-\infty}^{\infty} \int_0^{2\pi} |p\,(r\cos\varphi, r\sin\varphi, z)|\, d\varphi dz & \text{bounded as } r \to 0^+, \\ \boldsymbol{u} \cdot \boldsymbol{n} = \delta_t \boldsymbol{\eta} \cdot \boldsymbol{n} & \text{on } \Sigma_R, \\ -p\boldsymbol{n} = \lambda\, \nabla \boldsymbol{\eta}\, \boldsymbol{n} & \text{on } \Sigma_R, \\ \boldsymbol{\eta} \times \boldsymbol{n} = \boldsymbol{0} & \text{on } \Sigma_R, \\ \rho_s \delta_{tt} \boldsymbol{\eta} - \lambda \triangle \boldsymbol{\eta} = \boldsymbol{0} & \text{in } \Omega_s, \\ \gamma_{ST} \boldsymbol{\eta} + \lambda \nabla \boldsymbol{\eta}\, \boldsymbol{n} = P_{ext}\, \boldsymbol{n} & \text{on } \Sigma_{out}, \end{cases} \tag{1}$$

where ρ_f and ρ_s are the fluid and structure densities, λ the square of the wave propagation velocity, $\delta_t w := \frac{w - w^n}{\Delta t}$, $\delta_{tt} w := \frac{\delta_t w - \delta_t w^n}{\Delta t}$, $\Sigma_{out} = \{(x, y, z) \in \mathbb{R}^3 : x^2 + y^2 = (R + H)^2\}$, $\boldsymbol{n}$ is the unit vector orthogonal to the interfaces, and we have omitted the time index $n+1$. Problem $(1)_{1-3}$ is the fluid problem, problem $(1)_{7-8}$ is the structure problem equipped with a Robin condition at the external surface to model the elastic surrounding tissue, P_{ext} is the external pressure, whereas $(1)_{4-6}$ are the coupling conditions at the FS interface, stating the continuity of the velocities and of the tractions along the normal direction. The fluid and the structure problems have to be completed with initial conditions and with the assumption of decay to zero for $|z| \to \infty$.

By combining linearly $(1)_4$ and $(1)_5$ through the introduction of the linear operators $\mathcal{S}_f$ and $\mathcal{S}_s$ acting in the tangential direction to Σ_R, we obtain the following generalized Robin interface conditions (see Gigante and Vergara [2013])

$$\begin{cases} \mathcal{S}_f \Delta t\, \delta_t u_r - p = \dfrac{\mathcal{S}_f}{\Delta t}\, \eta_r + \lambda\, \partial_r \eta_r, \\ \dfrac{\mathcal{S}_s}{\Delta t}\, \eta_r + \lambda\, \partial_r \eta_r = \mathcal{S}_s \Delta t\, \delta_t u_r - p, \end{cases}$$

where $u_r = \boldsymbol{u} \cdot \boldsymbol{n}$ and $\eta_r = \boldsymbol{\eta} \cdot \boldsymbol{n}$, and where we have set to zero the terms at previous time steps since we analyze the convergence to the zero solution. Then, at time t^{n+1}, the corresponding iterative Schwarz method reads:

Given $\boldsymbol{u}^0, p^0, \eta^0$, solve for $j \geq 0$ until convergence

1. Fluid problem

$$\begin{cases} \rho_f \delta_t \boldsymbol{u}^{j+1} + \nabla p^{j+1} = \mathbf{0} & \text{in } \Omega_f, \\ \nabla \cdot \boldsymbol{u}^{j+1} = 0 & \text{in } \Omega_f, \\ \int_{-\infty}^{\infty} \int_0^{2\pi} |p\,(r\,\cos\varphi, r\,\sin\varphi, z)|\,d\varphi dz & \text{bounded as } r \to 0^+, \\ \mathcal{S}_f \Delta t\, \delta_t u_r^{j+1} - p^{j+1} = \dfrac{\mathcal{S}_f}{\Delta t}\,\eta_r^j + \lambda\,\partial_r \eta_r^j & \text{on } \Sigma_R; \end{cases} \tag{2}$$

2. Structure problem

$$\begin{cases} \rho_s \delta_{tt} \boldsymbol{\eta}^{j+1} - \lambda \triangle \boldsymbol{\eta}^{j+1} = \mathbf{0} & \text{in } \Omega_s, \\ \gamma_{ST} \boldsymbol{\eta}^{j+1} + \lambda \nabla \boldsymbol{\eta}^{j+1}\,\boldsymbol{n} = \mathbf{0} & \text{on } \Sigma_{out}, \\ \dfrac{\mathcal{S}_s}{\Delta t}\,\eta_r^{j+1} + \lambda\,\partial_r \eta_r^{j+1} = \mathcal{S}_s \Delta t\,\delta_t u_r^{j+1} - p^{j+1} & \text{on } \Sigma_R, \\ \boldsymbol{\eta}^{j+1} \times \boldsymbol{n} = \mathbf{0} & \text{on } \Sigma_R, \end{cases} \tag{3}$$

where we have set to zero the forcing term P_{ext} since we analyze the convergence to the zero solution.

By introducing the Fourier transform with respect to z and φ, and the symbols σ_f and σ_s related to $\mathcal{S}_f$ and $\mathcal{S}_s$, we can write the previous iterations with respect to the variables (r, m, k), where m is the discrete frequency variable related to the angular variable φ and k is the continuous frequency variable related to z. Then, we have the following

Proposition 1 *Set*

$$A(m,k) = -\frac{\lambda \Delta t \beta\,(K_m'(\beta\,R) - \chi\,I_m'(\beta\,R))}{K_m(\beta\,R) - \chi\,I_m(\beta\,R)}, \quad B(m,k) = -\frac{\rho_f\,I_m(kR)}{\Delta t\,k\,I_m'(kR)}, \tag{4}$$

where I_ν and K_ν are the modified Bessel functions, see Lebedev [1972]. Then, the reduction factor of iterations (2)-(3) *is given by*

$$\rho^j(m,k) \;=\; \rho(m,k) \;=\; \left| \frac{\sigma_f(m,k) - A(m,k)}{\sigma_s(m,k) - A(m,k)} \cdot \frac{\sigma_s(m,k) - B(m,k)}{\sigma_f(m,k) - B(m,k)} \right|, \tag{5}$$

where $\beta(k) = \sqrt{k^2 + \frac{\rho_s}{\lambda \Delta t^2}}$, and $\chi(m,k) := \frac{\gamma_{ST} K_m(\beta(R+H)) + \lambda\beta K_m'(\beta(R+H))}{\gamma_{ST} I_m(\beta(R+H)) + \lambda\beta I_m'(\beta(R+H))}$.

Moreover, the exact convergence set is given by $(\sigma_f, \sigma_s) \in \Theta_1(A,B) \cup \Theta_2(A,B)$, where

$$\Theta_1(A,B) = \left\{ (\sigma_f,\sigma_s) : \sigma_s < \sigma_f \text{ and } \left(\sigma_f - \tfrac{A+B}{2}\right)\left(\sigma_s - \tfrac{A+B}{2}\right) < \left(\tfrac{B-A}{2}\right)^2 \right\},$$
$$\Theta_2(A,B) = \left\{ (\sigma_f,\sigma_s) : \sigma_s > \sigma_f \text{ and } \left(\sigma_f - \tfrac{A+B}{2}\right)\left(\sigma_s - \tfrac{A+B}{2}\right) > \left(\tfrac{B-A}{2}\right)^2 \right\},$$

with A and B given by (4).

Proof. See Gigante and Vergara [2013].

3 Optimization procedure

From the previous results it follows that the reduction factor (5) is equal to zero for $\sigma_f^{opt} = A(m,k)$ and $\sigma_s^{opt} = B(m,k)$, with A and B given by (4). However, such choices are not implementable since they lead to non-local conditions. Then, a classical approach is to find the best values of the interface symbols within a suitable subset (Optimized Schwarz Method). In particular, in Gigante and Vergara [2013] it has been proposed to look for the best symbols belonging to a properly chosen curve parametrized with respect to a variable $p \in \mathbb{R}$, so that in fact we have a minimization problem over p. Let K be the set of the admissible frequencies. Then, we introduce the following quantities:

$$\overline{B} = \max_{(m,k)\in K} B(m,k)\,,\ \overline{A} = \min_{(m,k)\in K} A(m,k)\,,\ \overline{M} = \frac{1}{2}\left(\overline{A}+\overline{B}\right),$$
$$D(m,k) = \frac{1}{2}\left(A(m,k) - B(m,k)\right),\ M(m,k) = \frac{1}{2}\left(A(m,k) + B(m,k)\right),$$
$$Q(m,k) = \frac{\left|M(m,k) - \overline{M}\right|}{D(m,k)},\ \overline{Q} = \sup_{(m,k)\in K} Q(m,k)\,,\ N = \frac{\inf_{(m,k)\in K} D(m,k)}{\sup_{(m,k)\in K} D(m,k)}.$$

We have the following

Theorem 1. *Assume that $A(m,k)$ and $B(m,k)$ are bounded on K, with $B < A$ for all $(m,k) \in K$, and that $\overline{B} < \overline{A}$. Let*

$$\rho_0 = \max\left\{\left(\frac{1-\sqrt{N}}{1+\sqrt{N}}\right)^2;\left(\frac{1-\sqrt{1-\overline{Q}^2}}{\overline{Q}}\right)^2\right\}.$$

Then, for all $(m,k) \in K$, we have

$$\widehat{\rho}(p,m,k) = \left|\frac{p - A(m,k)}{2\overline{M} - p - A(m,k)}\,\frac{2\overline{M} - p - B(m,k)}{p - B(m,k)}\right| \le \rho_0,$$

if and only if $p \in [p_-, p_+]$ with

$$p_- = \overline{M} + \sup_{(m,k)\in K}\left\{\tfrac{1+\rho_0}{1-\rho_0} D(m,k) - \sqrt{\left(\overline{M} - M(m,k)\right)^2 + \tfrac{4\rho_0}{(1-\rho_0)^2}\left(D(m,k)\right)^2}\right\},$$
$$p_+ = \overline{M} + \inf_{(m,k)\in K}\left\{\tfrac{1+\rho_0}{1-\rho_0} D(m,k) + \sqrt{\left(\overline{M} - M(m,k)\right)^2 + \tfrac{4\rho_0}{(1-\rho_0)^2}\left(D(m,k)\right)^2}\right\}.$$

Proof. See Gigante and Vergara [2013].

The previous result tells us that moving along the line

$$\sigma_s = -\sigma_f + 2\overline{M}, \qquad \sigma_f \geq \overline{M},$$

it is possible to find a range of p which guarantees that the reduction factor is below a suitable value. This allows to choose properly the value of p in view of the numerical simulations.

4 Numerical results

In Gigante and Vergara [2013] we studied the numerical performance of the proposed estimates for a real fluid-structure interaction problem, inspired by haemodynamics, where the solution was characterized by radial symmetry, thus to a null dominant angular frequency m. In particular, we showed that in this case, the estimates provided by Theorem 1 allowed to choose effective values of the interface parameters.

Here we want to study some cases where the solution features non null dominant angular frequencies. In particular, we considered the coupling between the incompressible Navier-Stokes equations written in the Arbitrary Lagrangian-Eulerian formulation, see Donea [1982], and the linear infinitesimal elasticity, see for example Nobile et al. [2013], and we used a Robin-Robin partitioned procedure for its numerical solution, see Badia et al. [2008], Nobile and Vergara [2012]. In all the numerical experiments, we used the BDF scheme of order 1 for both the subproblems with a semi-implicit treatment of the fluid convective term. Moreover, we used the following data: $\rho_f = 1\, g/cm^3$, $\rho_s = 1.1\, g/cm^3$, $\gamma_{ST} = 3 \cdot 10^6\, dyne/cm^3$, fluid viscosity $\mu = 0.035\, dyne/cm^2$, Poisson ratio $\nu = 0.49$, Young modulus $E = 3 \cdot 10^6\, dyne/cm^2$. All these data are inspired from haemodynamic applications. We considered a cylinder with length $L = 5\, cm$, partitioned in an inner cylinder for the fluid problem with radius $R = 0.5\, cm$, 4680 tetrahedra and 1050 vertices, and an external cylindrical crown for the structure with thickness $0.1\, cm$ and 1260 vertices. For the numerical discretization, we used $P1bubble - P1$ finite elements for the fluid subproblem and $P1$ finite elements for the structure subproblem, and a time discretization parameter $\Delta t = 0.001\, s$. The space discretization parameter is $h = 0.25\, cm$, so that the frequency k varies in the range $[0.6, 12.5]$. In all the numerical experiments we prescribed the pressure $P_{in} = 1000\ dyne/cm^2$ at the inlet. All the numerical results have been obtained with the parallel Finite Element library `LIFEV` developed at MOX - Politecnico di Milano, INRIA - Paris, CMCS - EPF of Lausanne and Emory University - Atlanta.

We studied the following two cases, characterized by the following initial conditions for the velocity u_{0z} along the z direction:

1.

$$u_{0z}(x,y) = 10^3\left(x^5 - 10x^3y^2 + 5xy^4\right)\ cm/s = 10^3 r^5\cos(5\varphi)\,cm/s. \quad (6)$$

In this case the leading frequency is $m = 5$ and therefore we apply Theorem 1 with $m = 5$ and $0.6 \leq k \leq 12.5$, obtaining $\rho_0 = 0.05$, provided that $p \in [6684, 9586]$, with $\overline{M} = 3651$;

2.

$$u_{0z}(x,y) = \begin{cases} 10\left(x^2+y^2\right)\frac{\sin\left(10.5\arctan\left(\frac{y}{x}\right)\right)}{\sin\left(0.5\arctan\left(\frac{y}{x}\right)\right)} & cm/s \quad x>0, y\neq 0, \\ 210x^2 & cm/s \quad x>0, y=0, \\ 10\left(x^2+y^2\right)\frac{\cos\left(10.5\arctan\left(\frac{y}{x}\right)\right)}{\cos\left(0.5\arctan\left(\frac{y}{x}\right)\right)} & cm/s \quad x<0, \\ -10y^2 & cm/s \quad x=0. \end{cases} \quad (7)$$

$$= 10r^2\left(1 + 2\sum_{m=1}^{10}\cos(m\varphi)\right)\ cm/s.$$

This function is the Dirichlet kernel which is characterized by the fact that all the frequencies m between 0 and 10 are equally distributed. We then apply Theorem 1 with $0 \leq m \leq 10$ and $0.6 \leq k \leq 12.5$, obtaining $\rho_0 = 0.32$, provided that $p \in [1983, 7521]$, with $\overline{M} = 1323$.

Of course we prescribe the same initial condition for the displacement $\boldsymbol{\eta}$ along the z direction.

In both the cases the solution is supposed to feature, at least for the first time steps, the same leading frequencies as the initial condition, so that the application of the estimates provided by Theorem 1 are supposed to lead to excellent convergence properties. In particular, we run the numerical experiments for two time steps, that is we set $T = 0.002\,s$ as the final instant.

In Figure 1 we depict the computed velocity along the z direction after the first time step.

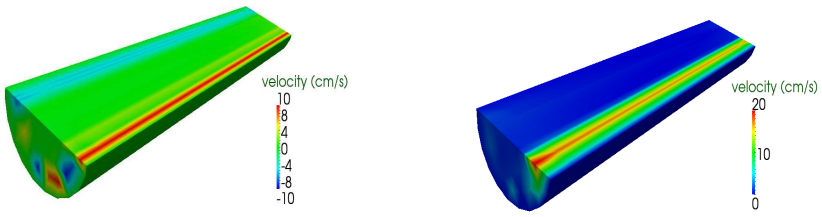

Fig. 1 Velocity along the z direction after the first time step. Left: case characterized by $m = 5$ as the leading frequency; Right: Dirichlet kernel.

We run the numerical simulations for a wide range of the parameter p. We found that the optimal value is $p = 9000$ for the first case and $p = 3000$ for the second case. In Tables 1 and 2, we report the mean number of iterations for some of the couples of the interface parameters used in the numerical simulations, some of them within the range estimated by Theorem 1 and some of them outside such a range.

σ_f/σ_s	u_{0z} given by (6)	σ_f/σ_s	u_{0z} given by (7)
6684/618	24.5	1000/-1646	X
8000/-698	12.0	**1983/663**	9.5
9000/-1698	8.5	**3000/-354**	4.5
9586/-2284	8.5	**5000/-2354**	8.0
12000/-4698	10.0	**7521/-4875**	10.5
15000/-7698	13.5	10000/-7354	13.0

Table 1 Values of the interface parameters and mean number of iterations over the two time steps for the initial condition given by (6) (left) and by (7) (right). In bold the couples of σ_f and σ_s within the optimal range estimated by Theorem 1. X means that no convergence has been achieved.

These numerical results show that the optimal value of p falls in both the cases within the range estimated by Theorem 1 and that outside such a range the convergence properties deteriorate. In particular, we observe that the performance worsens faster going towards the left extreme of the optimal range. This could be explained by looking at Figure 4, left, in Gigante and Vergara [2013], where it could be observed that the level sets are denser for small values of σ_f and σ_s (that is of p), so that the performance is more sensitive to small perturbation of p when p is small.

In conclusion, our results showed the effectiveness of the estimates provided in Gigante and Vergara [2013] also when the dominant angular frequencies are different from zero.

References

S. Badia, F. Nobile, and C. Vergara. Fluid-structure partitioned procedures based on Robin transmission conditions. *Journal of Computational Physics*, 227:7027–7051, 2008.

V. Dolean, M.J. Gander, and L. Gerardo Giorda. Optimized Schwarz Methods for Maxwell's equations. *SIAM Journal on Scientific Computing*, 31(3): 2193–2213, 2009.

J. Donea. An arbitrary Lagrangian-Eulerian finite element method for transient dynamic fluid-structure interaction. *Computer Methods in Applied Mechanics and Engineering*, 33:689–723, 1982.

M.J. Gander. Optimized Schwarz Methods. *SIAM Journal on Numerical Analysis*, 44(2):699–731, 2006.

M.J. Gander, F. Magoulès, and F.Nataf. Optimized Schwarz methods without overlap for the Helmholtz equation. *SIAM Journal on Scientific Computing*, 24:38–60, 2002.

L. Gerardo Giorda, F. Nobile, and C. Vergara. Analysis and optimization of Robin-Robin partitioned procedures in fluid-structure interaction problems. *SIAM Journal on Numerical Analysis*, 48(6):2091–2116, 2010.

G. Gigante and C. Vergara. Analysis and optimization of the generalized Schwarz method for elliptic problems with application to fluid-structure interaction. Report n. 04-2013, Dipartimento di Ingegneria, Università di Bergamo, Italy, 2013.

G. Gigante, M. Pozzoli, and C. Vergara. Optimized Schwarz Methods for the diffusion-reaction problem with cylindrical interfaces. *SIAM Journal on Numerical Analysis*, 51(6):3402–3420, 2013.

C. Japhet. Optimized Krylov-Ventcell method. Application to convection-diffusion problems. In P.E. Bjorstad, M.S. Espedal, and D.E. Keyes, editors, *Proceedings of the Ninth International Conference on Domain Decomposition Methods*, pages 382–389, 1998.

C. Japhet, N. Nataf, and F. Rogier. The optimized order 2 method. Application to convection-diffusion problems. *Fut Gen COmput Syst*, 18:17–30, 2001.

N. Lebedev. *Special Functions and Their Applications*. Courier Dover Publications, 1972.

P.L. Lions. On the Schwartz alternating method III. In T. Chan, R. Glowinki, J. Periaux, and O.B. Widlund, editors, *Proceedings of the Third International Symposium on Domain Decomposition Methods for PDE's*, pages 202–223. Siam, Philadelphia, 1990.

F. Nobile and C. Vergara. Partitioned algorithms for fluid-structure interaction problems in haemodynamics. *Milan Journal of Mathematics*, 80(2): 443–467, 2012.

F. Nobile, M. Pozzoli, and C. Vergara. Time accurate partitioned algorithms for the solution of fluid-structure interaction problems in haemodynamics. *Computer & Fluids*, 86:470–482, 2013.

A. Qaddouria, L. Laayounib, S. Loiselc, J Cotea, and M.J. Gander. Optimized Schwarz methods with an overset grid for the shallow-water equations: preliminary results. *Appl. Num. Math*, 58:459–471, 2008.

B. Stupfel. Improved transmission conditions for a one-dimensional domain decomposition method applied to the solution of the Helmhotz equation. *Journal of Computational Physics*, 229:851–874, 2010.